A model for the net-baryon rapidity distribution

R. Conceição*, J. Alvarez-Muñiz†, J. Dias de Deus‡§, M.C. Espírito Santo*‡, J. G. Milhano‡§ and M. Pimenta*‡

*LIP, Av. Elias Garcia, 14-1, 1000-149 Lisboa, Portugal
†IGFAE and Dep. Fisica Particulas, Univ. Santiago de Compostela, 15782 Santiago de Compostela, Spain
‡Departamento de Física, IST, Av. Rovisco Pais, 1049-001 Lisboa, Portugal
§CENTRA, Av. Rovisco Pais, 1049-001 Lisboa, Portugal

Abstract. **In nuclear collisions, a sizable fraction of the available energy is carried away by baryons. As the baryon number is conserved, the net-baryon $\mathrm{B}-\bar{\mathrm{B}}$ retains information on the energy-momentum carried by the incoming nuclei. A simple and consistent model for net-baryon production in high energy proton-proton and nucleus-nucleus collisions is presented. The basic ingredients of the model are valence string formation based on standard PDFs with QCD evolution and string fragmentation via the Schwinger mechanism. The results of the model are presented and compared with data at different centre-of-mass energies and centralities. These results show that a good description of the main features of net-baryon data is possible in the framework of a simplistic model, with the advantage of making the fundamental production mechanisms manifest.**

Keywords**: Hadronic collisions, net-baryon rapidity distribution, valence strings**

I. The model

In this paper we present a simple and consistent model for net-baryon production in high energy proton-proton (p-p) and nucleus-nucleus (A-A) collisions. A detailed description of the model, as well as a more detailed comparison with data and Monte Carlo models can be found in [1].

In the spirit of [2], [3], [4], the basic assumption of our model is that net-baryon production in proton-proton collisions is strongly correlated with the formation and fragmentation of two color singlet strings, each with two valence quarks from one of the protons, and one valence quark from the other proton. This is schematically shown in figure 1.

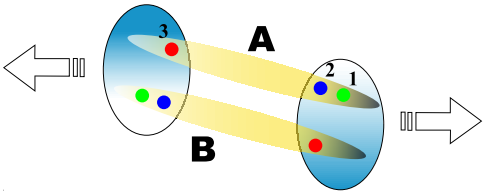

Fig. 1. Schematic representation of a proton-proton collision, with the formation of two valence strings.

Referring to the figure, let x_1, x_2 and x_3 be the fractions of momentum carried by the valence quarks forming string A. Quarks 1 and 2 are from the proton with positive momentum in the proton-proton reference frame, and quark 3 is from the other proton. No transverse momentum is considered within this model. By choice, $x_1 > x_2 > x_3$, with $x_3 < 0$. The energy and momentum of each string are obtained adding directly the energy and momentum carried by each of the valence quarks. For string A:

$$E_{string} = (x_1 + x_2 + (-x_3))\frac{\sqrt{s}}{2}, \quad (1)$$

$$P_{string} = (x_1 + x_2 - (-x_3))\frac{\sqrt{s}}{2}, \quad (2)$$

$$M_{string} = \sqrt{(x_1 + x_2)\ (-x_3)\ s}, \quad (3)$$

where the quark momentum fractions x_1, x_2 and x_3 are determined from the valence quark PDFs at an effective momentum scale Q^2. For each $\sqrt{s}$, an effective Q^2 derived from a fit to experimental data will be chosen (see next section). In this work the CTEQ6M parton distribution functions [5] were used.

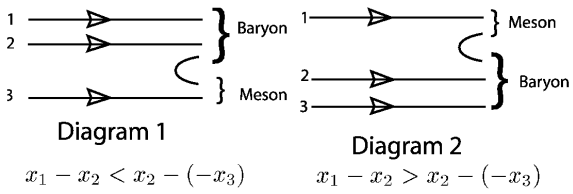

Fig. 2. The two main valence string fragmentation diagrams. In the simple model assumed, the string is cut in two pieces and a $q\bar{q}$ pair is formed, from the vacuum, between the two quarks with the largest momentum difference. See text for details.

The simplest possible model for fragmentation is assumed. Each string decays into a baryon and a meson in the following way: the string is cut in two pieces and a $q\bar{q}$ pair is formed, from the vacuum, either between quarks 2 and 3 (belonging to different protons) or between quarks 1 and 2 (belonging to the same proton, with positive momentum in the case of string A). The quark pair with the largest momentum difference is chosen. The string piece that inherits two valence quarks originates the baryon, whereas the string piece that inherits one valence quark originates the meson. This mechanism corresponds to the diagrams represented in figure 2. Diagram 1 corresponds to the case $x_1 - x_2 < x_2 - (-x_3)$, in which quarks 2 and 3 are chosen.

In Diagram 2, $x_1 - x_2 > x_2 - (-x_3)$ and string fragmentation occurs between quarks 1 and 2.

The relative weights of the two diagrams are, in this model, given only by kinematics. For string A the first diagram will be more probable (especially for low $\sqrt{s}$). However, the weight of the second diagram can be as large as 40% above LHC energies.

The $q\bar{q}$ pair formed from the vacuum was taken to be either a $u\bar{u}$ or a $d\bar{d}$, and the full quark combinatorics was then performed in order to determine the nature of the possible outcoming baryon. Both fundamental and excited states were considered, taking spin-dependent weights $(2j+1)$. The decays of the unstable baryons were then performed and the outcoming nucleons included in the net-baryon calculations. The contribution from s quarks was not considered.

In this model the net-baryon rapidity $(dn/dy)^{B-\bar{B}}$ in proton-proton collisions is thus obtained from the rapidity of the two baryons produced in the fragmentation of the valence strings, having the effective momentum scale Q^2 at each $\sqrt{s}$ as the only free parameter.

Let us now consider the case of A-A collisions. The net-baryon results depend directly on the collision centrality. The number of participants will thus play an important role in the model. We shall assume that the net-baryon rapidity in A-A collisions at a given $\sqrt{s}$ can be obtained from the net-baryon rapidity in p-p collisions at the same $\sqrt{s}$ computed at an effective Q_A^2 value which depends both on $\sqrt{s}$ and on A, with a normalisation factor which is the number of participants per nucleus, $N_{part}/2$:

$$\left.\frac{dn}{dy}^{B-\bar{B}}(Q_A^2)\right|_{A-A} \simeq \frac{N_{part}}{2}\cdot\left.\frac{dn}{dy}^{B-\bar{B}}(Q_A^2)\right|_{p-p}, \quad (4)$$

where both rapidity distributions are evaluated at Q_A^2. As stated above, the model does not include $s\bar{s}$ pairs. We are thus assuming that strangeness does not considerably distort the distribution.

When comparing to net-proton results, we consider that net-proton is roughly half of $(B-\bar{B})$ [10]. As strangeness effects are not included in the model, the obtained rapidity distribution is well suited for comparing to data with weak decay corrections included. The strangeness effect is in this case simply a global factor ε_s, estimated from the Schwinger model to be about 25% to 35%, which can be included in the normalisation factor:

$$\left.\frac{dn}{dy}^{p-\bar{p}}(Q_A^2)\right|_{A-A} \simeq \frac{N_{part}}{4}\cdot(1-\varepsilon_s)\cdot\left.\frac{dn}{dy}^{B-\bar{B}}(Q_A^2)\right|_{p-p}. \quad (5)$$

Nuclear effects correction factors for the valence quark PDFs were estimated, using EKS98 [6] and nDS [7], to be below 10-15% and taken into account in the calculations.

To address the energy evolution of the model, a relation between the effective Q^2 and $\sqrt{s}$ needs to be established. The effective Q^2 corresponds to the typical transverse size (area) of the parton. It is reasonable to assume, as in Regge phenomenology [8], that the average number of partons in a nucleon increases as a power of the centre of mass energy $\sqrt{s}$. Thus, $R_h^2 Q^2 \sim \sqrt{s}/\sqrt{s_0}$, where R_h is the nucleon radius which we take as fixed. It then follows that Q^2 should grow, allowing for deviations from this naïve expectation, according to

$$Q^2 = Q_0^2\left(\frac{s}{s_0}\right)^{\lambda_v}\left[GeV^2\right]. \quad (6)$$

Further, the effective Q_A^2, for A-A, should be analogously related to $\sqrt{s}$, but account for an extra dependence on the number of participants. Since the number of partons involved in an A-A collision grows proportionally to the number of nucleons from each nucleus involved in the collision (i.e. $\propto N_{part}/2$) and the transverse size (area) of the nucleus grows proportionally to $(N_{part}/2)^{2/3}$, we can expect the typical inverse size of a parton Q_A^2 to grow proportionally to $(N_{part}/2)^{1/3}$. Also, we can expect this simple geometrical estimate to be modified by nuclear effects and thus write for the A-A effective Q_A^2, as a function of the p-p effective Q^2:

$$Q_A^2 = \left(\frac{N_{part}}{2}\right)^{\alpha} Q^2. \quad (7)$$

The value of α will be estimated using the data at different centralities available for $\sqrt{s} \simeq 17$ GeV.

Combining equations (6) and (7), we can thus write, for A-A collisions:

$$Q_A^2 = Q_0^2\left(\frac{N_{part}}{2}\right)^{\alpha}\left(\frac{s}{s_0}\right)^{\lambda_v}\left[GeV^2\right], \quad (8)$$

where the exponent λ_v will be estimated performing a fit to the available data points. Below, the free parameters of the model will be fixed by adjusting the results of the model to the experimental data at each $\sqrt{s}$ and centrality.

II. Results

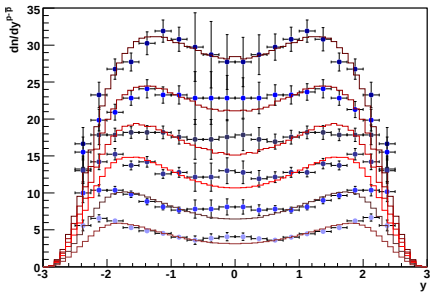

Fig. 3. The results of the model for net-proton rapidity are compared to NA49 data in different centrality ranges (from top to bottom: 0-5%, 5-14%, 14-23%, 23-31%, 31-48% and 48-100%.) [9].

The experimental results are presented in terms of net-baryon rapidity in the case of BRAHMS and in terms of net-proton rapidity in the case of NA49 and of the AGS experiments. The model calculations are performed

using equation (4) for the net-baryon case and (5) for the net-proton one.

The NA49 net-proton rapidity distributions for different centrality ranges at $\sqrt{s} \simeq 17$ GeV presented in [9] were used in the first step of this analysis. Our model was fitted to these data points in each centrality bin, taking as free parameters the effective Q_A^2 and a normalisation factor n. The data points and the results of the model are shown in figure 3. A satisfactory agreement is achieved for all the centrality ranges. The apparent difference between data and the model in the mid-rapidity region, could be due to the fact that the experimental error bars do not include the error associated to weak corrections. On the other hand, difractive effects are not included in the model. This accounts for the poorer description of the high rapidity extremes in peripherial collisions. It is worth noting that the effect seen in data, displacing the maxima of the distribution to higher rapidity values as the centrality of the collision decreases, is reproduced in the model through a decrease of the fitted Q_A^2 value.

The normalisation factor n obtained from the fit was compared with what would be expected from equation (5) using the number of participants estimated by the experiment in [9] and assuming $\varepsilon_s = 0.25$. A good agreement was found. The relation between n and N_{part} is thus well understood, giving us confidence on the model and on the fitting procedure.

We thus have, for each centrality, a number of participants and a value of Q_A^2. These results can be used to estimate the exponent α on equation (7), which relates the effective Q^2 in p-p and A-A collisions. This was done by fitting equation (7) to these (Q_A^2, N_{part}) points, leaving Q^2 and α as free parameters. The best fit is the one with $\alpha = 0.53^{+0.12}_{-0.13}$.

Turning now to the evolution with $\sqrt{s}$, we consider the results available for central collisions at RHIC, the SPS and AGS [9], [10], [11], [12], [13]. As above, in order to fully define the model we need to choose an effective Q_A^2 value and a normalisation factor related to N_{part} (and to ε_s, in the case of net-proton). In practice, this was done by fitting the model predictions to the existing rapidity data using as free parameters the effective Q^2 (and assuming the relation to Q_A^2 we have just inferred from centrality data) and a normalisation factor n. The data points and the results of the fit are shown in figure 4. A good description of the existing data is achieved. At $\sqrt{s} \simeq 5$ GeV only the points up to the nominal beam rapidity were considered, since our model does not include low energy effects, such as Fermi momentum effects, and therefore has no mechanism to reproduce these data. At the other centre-of-mass energies all data points were included in the fit. The present RHIC data at $\sqrt{s} = 200$ GeV cover only the mid-rapidity range, leaving the fit largely unconstrained. For this reason, at this centre-of-mass energy the normalisation factor was fixed to the value estimated in reference [10] and only Q^2 was left as a free parameter. In all the other cases

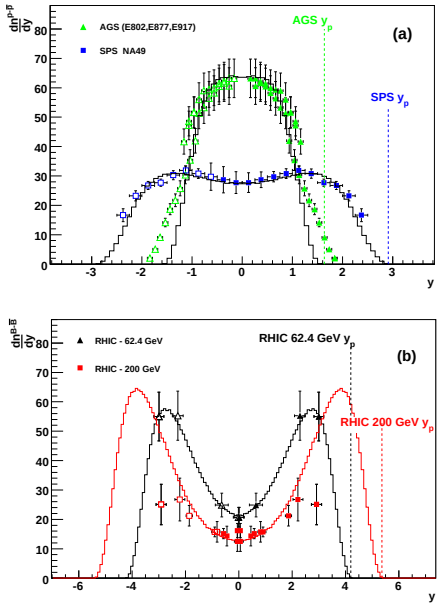

Fig. 4. The results of the present model for: (a) net-proton and (b) net-baryon rapidity are compared to experimental data from central A-A collisions at different centre-of-mass energies. See [10], [11], [12], [13] for details on the data points.

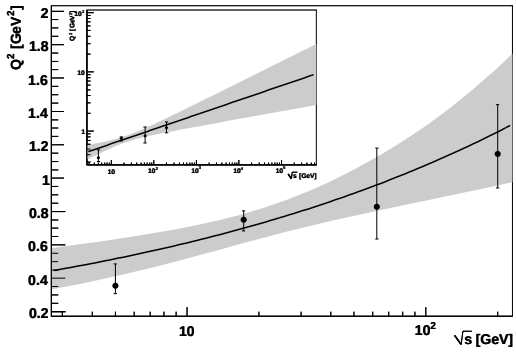

Fig. 5. The effective Q_A^2 values at different centre-of-mass energies chosen by tuning the model to the experimental data are shown. The line shows the fit using eq. (8) and considering Au-Au collisions. The shaded areas correspond to 1σ variations of the fit parameters.The inset figure shows the extrapolation of the fit to higher energies, covering the LHC and very high energy cosmic rays.

the normalisation was left free.

The values obtained for the effective Q^2, the normalisation factor n and the number of participants N_{part} (computed from equations (4) and (5)) are given in table I, where the number of participants estimated by the experiments [9], [10], [11], [13] for the relevant centrality region is also given. The fitted N_{part} values are in good agreement with the expectations. The discrepancy at $\sqrt{s} = 5$ GeV is due to the effect in the normalisation factor of excluding the points above the nominal centre-of-mass energy from the fit.

Assuming that equation (8) describes the evolution of the effective Q_A^2 with centrality and $\sqrt{s}$, the exponent λ_v

TABLE I
RESULTS OF THE FIT TO THE Q^2 AND THE NORMALISATION FACTOR n AT THE DIFFERENT ENERGIES. THE NUMBER OF PARTICIPANTS OBTAINED FROM EQUATIONS (4) AND (5) (N_{part}) AND ESTIMATED BY THE EXPERIMENTS (N_{part}^{Ref}) ARE ALSO GIVEN.

$\sqrt{s}$ (GeV)	Q^2 (GeV^2)	n	N_{part}	N_{part}^{Ref}
5 (Au-Au)	$0.35^{+0.13}_{-0.05}$	$66.6^{+2.4}_{-3.1}$	$266.4^{+9.6}_{-12.4}$	344 ± 6
17 (Pb-Pb)	$0.76^{+0.05}_{-0.07}$	$67.7^{+1.4}_{-1.4}$	$361.1^{+7.5}_{-7.5}$	362 ± 12
62.4 (Au-Au)	$0.77^{+0.33}_{-0.18}$	$148.2^{+12.6}_{-12.4}$	$296.4^{+25.2}_{-24.8}$	314 ± 8
200 (Au-Au)	$1.14^{+0.29}_{-0.20}$	–	–	357 ± 8

was determined by fitting this equation to the $(\sqrt{s}, Q^2)$ points in table I. This is shown in figure 5, where the points are the Q^2 values adjusted above, the line is the fit to these points with equation (8) and the shaded areas correspond to 1σ variations of the fit parameters. The value obtained for the exponent was $\lambda_v = 0.25^{+0.12}_{-0.11}$, taking $\sqrt{s_0} \simeq 17$ GeV.

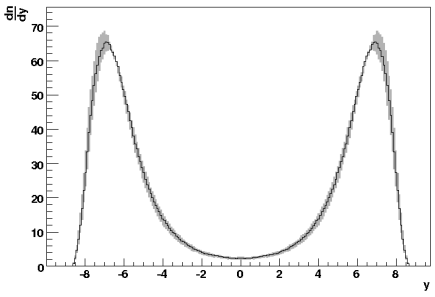

Fig. 6. Predictions of the model for net-baryon rapidity for central Pb-Pb collisions at $\sqrt{s} = 5.5$ TeV

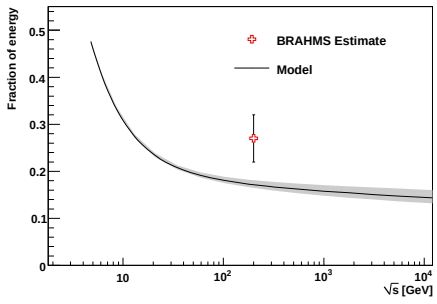

Fig. 7. Evolution of the fraction of energy carried by the net-baryon with $\sqrt{s}$. The prediction of the present model (with a shaded band corresponding to the 1σ variation of the fit parameters) for Au-Au collisions with a 5% centrality cut are shown and compared to the RHIC estimate given in [14].

The predictions of the present model for net-baryon rapidity at higher centre-of-mass energies were then obtained and are shown in figure 6. The width of the curves corresponds to varying the Q^2 within the 1σ band shown in figure 5. In figure 6(a) the net-baryon rapidity distribution in central Pb-Pb collisions at $\sqrt{s} = 5.5$ TeV is presented. Following reference [15], the number of participants corresponding to selecting the 6% most central collisions was set.

Finally, the fraction of the centre-of-mass energy carried by the net-baryon as a function of $\sqrt{s}$ was computed and is shown in figure 7 (together with the 1σ bounds). The prediction is for Au-Au central collisions. According to [14], RHIC data indicate about 27% of the initial energy remaining in the net-baryon after the collision. At higher energies, a sizable amount of energy is still associated to the net-baryon.

III. SUMMARY AND CONCLUSIONS

A simple and consistent model for net-baryon production in high energy proton-proton and nucleus-nucleus collisions was presented.

The free parameters in the model (the effective Q^2 and the number of participating nucleons) were fitted to the available data. The results show that a good description of the main features of net-baryon data is achieved on the basis of this simple model, in which the fundamental production mechanisms appear in a transparent way.

The model predicts that a sizable amount of energy may be associated to the net-baryon, even at high energies.

IV. ACKNOWLEDGEMENT

R. Conceição is supported by grant SFRH / BD / 30706 / 2006 from FCT.

REFERENCES

[1] DOI: 10.1140/epjc/s10052-009-1029-8
[2] L. Van Hove, S. Pokorski, Nucl. Phys. B 86 (1975) 245; L. Van Hove, Acta Phys. Pol. B 7 (1976) 339.
[3] R.P. Feynman, Phys. Rev. Lett. 23 (1969).
[4] A. Capella, U. Sukhatme, C.-I. Tan, J. Tran Thanh Van, Phys.Rept. 236 (1994) 225-329.
[5] J. Pumplin, D.R. Stump, J.Huston, H.L. Lai, P. Nadolsky, W.K. Tung, JHEP 0207 (2002) 012; D. Stump, J. Huston, J. Pumplin, W.K. Tung, H.L. Lai, S. Kuhlmann, J. Owens, JHEP 0310 (2003) 046; S. Kretzer, H.L. Lai, F. Olness, W.K. Tung, Phys. Rev. D 69(2004) 114005.
[6] K.J. Eskola, V.J. Kolhinen and C.A. Salgado, Eur. Phys. J. C. 9 (1999) 61; K.J. Eskola, V.J. Kolhinen and P.V. Ruuskanen, Nucl. Phys. B 535 (1998) 351.
[7] D. de Florian, R. Sassot, Phys. Rev. D 69 (2004) 074028.
[8] V.A. Abramovsky, E.V. Gedalin, E.G. Gurvich, O.V. Kancheli, Sov. J. Nucl. Phys. 53 (1991) 172-176; N.S. Amelin, N. Armesto, C. Pajares, D. Sousa, Eur. Phys. J. C 22 (2001) 149-163.
[9] D. Röhrich for the NA49 Collab., Nucl. Phys. A 663 & 664 (2000) 713c; G. E. Cooper for the NA49 Collab., Nucl. Phys. A661 (1999) 362c.
[10] BRAHMS Collab., I.G. Bearden et. al., Phys. Rev. Lett. 93 (2004) 102301.
[11] BRAHMS Collab., I.C. Arsene et. al., arXiv:0901.0872v1 [hep-ex], submitted to Phys. Rev. Lett. B.
[12] NA49 Collab., H. Appelshauser et al., Phys. Rev. Lett. 82 (1999) 2471.
[13] E802 Collab., L. Ahle et al., Phys. Rev. C 60 (1999) 064901; E877 Collab., J. Barette et al., Phys. Rev. C 62 (2000) 024901; E917 Collaboration, B.B. Back et al., Phys. Rev. C 66 (2002) 054901.
[14] B.B. Back, Phys. Rev. C 72 (2005) 064906.
[15] D. Kharzeev, E. Levin and M. Nardi, Nucl. Phys. A 747 (2005) 609.